PHYSICAL REVIEW B VOLUME 20, NUMBER 5 1 SEPTEMBER 1979

Electron-energy-loss spectra of vanadium, niobium, molybdenum, and tantalum

W. K. Schubert and E. L. Wolf
Ames Laboratory-U.S. Department of Energy and Department of Physics,
Iowa State University, Ames, Iowa 50011

(Received 8 May 1979)

Electron-energy-loss spectra were obtained out to approximately 80 eV in the reflection mode from atomically clean foil samples of vanadium, niobium, molybdenum, and tantalum. Results are compared with previous ultraviolet optical work and electron-energy-loss spectroscopy (ELS) studies on these materials. Resolution of structure is improved over many previous ELS investigations by using synchronous detection techniques in determining energy locations. Origins of the various observed structures are discussed in light of previous studies, particularly ultraviolet optical work leading to the determination of the complex dielectric function. We comment on discrepancies existing in the literature about plasmon energies in these materials estimated from infrared optical measurements.

I. INTRODUCTION

The considerable current interest in the transition metals, and particularly their electronic properties, arises in part from their occurrence in high-critical-temperature elemental and compound superconductors. The highest elemental transition temperature is found in niobium (9.2 °K),[1] and the highest known transition temperatures are found in the *A*-15 compounds of niobium and vanadium.[1] While the existence of high transition temperatures has long been established, understanding of the underlying mechanisms is not so well developed. Superconductivity in these materials is generally believed to arise from the electron-phonon interaction described by a basic coupling parameter $\lambda = N(0)\langle I^2\rangle / M\langle\omega^2\rangle$,[2] where $N(0)$ is the density of states of one spin index at the Fermi energy, $\langle I^2\rangle$ is an averaged, squared electron-phonon matrix element, M is the ionic mass, and $\langle\omega^2\rangle$ is a particular average of the phonon spectrum. The numerator in λ depends on the electronic structure near the Fermi energy in a complex and incompletely understood fashion. Thus, it is of timely interest to study more intensively the electronic properties of these materials.

In particular, it seems of interest to experimentally examine the collective electron behavior represented by the plasma oscillations for three reasons. First, the question of screening of the electron-phonon interaction by collective electron motion is regarded[3] as a central difficulty in the accurate calculation of λ. Second, there is the recent restatement[4] of Frölich's suggestion[5] that screening of *d*-electron plasma oscillations by *s* electrons in transition metals (and their compounds) may allow the formation of an acoustic plasmon branch which could in principle supplement or replace the electron-phonon interaction leading to superconductivity. Third, the collective properties, in contrast to one-electron properties which are reasonably predicted by existing band-structure calculations, seem to present greater difficulty in theoretical calculations. We make this statement because recent theoretical calculations of plasma energies[6,7] in niobium are not in agreement with energy-loss spectroscopy (ELS) or uv optical studies. In addition, infrared absorption work[7,8] on niobium yields plasma energies which also are not in agreement with ELS or uv optical studies.

Electron-energy-loss spectroscopy measures, in principle, the volume and surface loss functions[9] defined in the dielectric theory as

$$\mathrm{Im}\left(-\frac{1}{\tilde{\epsilon}}\right) = \text{Volume loss function} \ , \tag{1}$$

$$\mathrm{Im}\left(-\frac{1}{\tilde{\epsilon}+1}\right) = \text{Surface loss function} \ , \tag{2}$$

where $\tilde{\epsilon} = \epsilon_1 + i\epsilon_2$ is the complex dielectric function. In transmission ELS, one expects to see primarily volume excitations and thus measure the volume loss function. In contrast, reflection ELS is expected to be more surface sensitive and thus measure the surface loss function. Experimentally, however, the volume and surface contributions are not completely separated in the different modes.[9,10] Indeed, in a comparison of the present reflection ELS results with loss functions determined optically,[11,12] (Fig. 1) both volume and surface features are apparent.

Experimental constraints have dictated the use of reflection rather than transmission ELS in the present study. In surface studies, it is highly desirable to make and study samples *in situ* under ultrahigh vacuum. This helps to insure surface cleanliness, and in particular, minimizes the presence of oxide layers which can result in altered ELS spectra.[13,14] This experimental requirement makes the use of transmission ELS impractical, as very thin (≲200 Å), free-standing samples are required, which in practice, must be prepared outside the analysis vacuum chamber.

While experimentally cleaner and more convenient, reflection ELS does require more care in spectral interpretation. One measures experimentally $N(E)$, the number of electrons suffering energy loss E upon interacting with the sample. The method is most useful if one can establish that a loss E involves only a single scattering event. This assumption is most clearly valid in transmission ELS conducted on very thin samples with high-incident electron energy (20–50 keV) and at very small deflection angles. In reflection ELS, electrons are strongly scattered (reflected) by the sample. However, a sharp elastic peak (at $E=0$) is observed, and it appears that a significant fraction of the scattered electrons can be associated with single *inelastic* events (as in high-energy transmission ELS) occurring in combination with a purely *elastic* reflection. Indeed, one objective of the present study is to demonstrate empirically a one-to-one mapping of spectral features in the low-energy region of reflection ELS into peaks in the volume and surface-loss functions determined from comprehensive optical studies.[11,12]

Reduction of the effects of a multiple-scattering background on the energy location of structure in $N(E)$ is achieved in the present study by experimen-

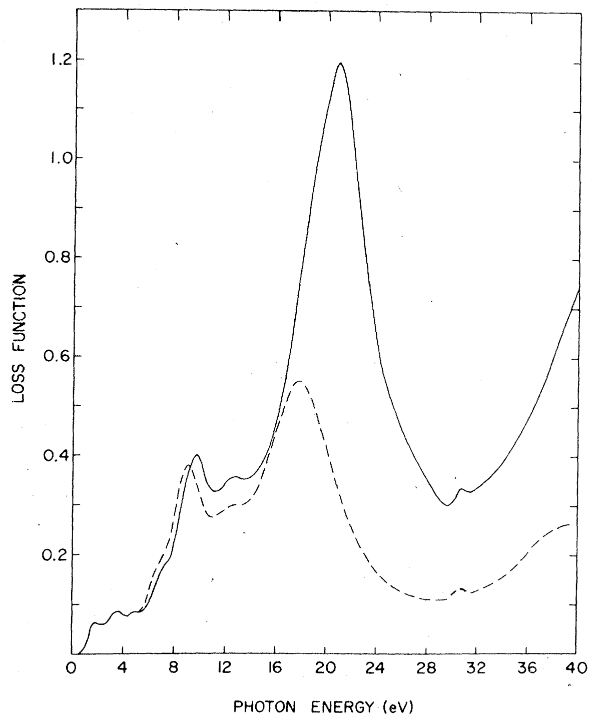

FIG. 1. Volume and surface loss functions of niobium as determined by Weaver *et al.* (Ref. 12) from ultraviolet optical studies. The volume function $\mathrm{Im}(-1/\tilde{\epsilon})$ is shown as a solid line; the surface function $\mathrm{Im}[-1/(\tilde{\epsilon}+1)]$, dashed. (From Ref. 12, with permission.)

TABLE I. Vanadium.

		Energy loss (eV)[a]							
		A	B	C	D	E	E′	E″	F
Reflection ELS	This study	5.3 ± 0.1	9.6 ± 0.2	14.8 ± 0.2	21.5 ± 0.2	36.6 ± 0.5	39.2 ± 0.5	47.4 ± 0.5	66.9 ± 0.5
	Ref. 18	5.0	9.4	14.0	22.0	37.2	39.7	44	67.2
	Ref. 14	5.1	10.5	16.5	24.0				
	Ref. 22	5.8	12.5		22.1		42	48	67.4
	Ref. 23	5.4			21.6		41.9	51.6	67.4
	Ref. 24	5.1	10.3	14.3	20	37.8		47.6	66.6
Transmission ELS	Ref. 10	5.6	11.0		21.5		39	45.7	
uv optical	Ref. 11[b]	5.2	11.0	10.0	18.4				
X-ray atomic energy levels	Ref. 25					37.8 ± 0.3 $M_{\mathrm{II,III}}$			66.5 ± 0.4 M_{I}
Calculated free electron $\hbar\omega_p$	Ref. 11				22.3				

[a] Here and in the following tables A and C are surface plasmons, B and D are volume plasmons, and further lettered structures E, F, etc., are core-level excitations. Primes denote features which are not completely understood. Notation for atomic core levels follows Bearden and Burr, Ref. 25.

[b] Authors felt data were affected by surface oxide.

TABLE II. Niobium.

		Energy loss (eV) A	B	C	D	E	E′	F
Reflection ELS	This study	9.6 ±0.1		18.3 ±0.2	20.8 ±0.3	30.3 ±0.4	37.9 ±0.4	57.9 ±0.5
	Ref. 21	9.5		19.6		32.4	42.0	62.4
	Ref. 33[a]	10.2(GI)		17.2(GI)		34.6(GI)	41(GI)	54.3(GI)
		10.2(NI)		19.8(NI)		34.6(NI)	42(NI)	55.2(NI)
	Ref. 34	9.9		19.7				
uv optical	Ref. 12	9.0	9.7	17.7	20.8			
X-ray atomic energy levels	Ref. 25					33.9 ±0.4 $N_{\mathrm{II}},N_{\mathrm{III}}$		58.1 ±0.3 N_{I}
Calculated free Electron $\hbar\omega_p$	Ref. 11				19.6			

[a]GI: Grazing incidence, NI: normal incidence.

tally measuring derivatives of $N(E)$ through use of synchronous detection. In the low-energy region ($E \lesssim 30$ eV), maxima in $N(E)$ are located by peaks in $-N''(E) = -d^2N/dE^2$. The second derivative discriminates against linearly or quadratically rising backgrounds, in that these would provide, respectively, no contribution or simply a constant contribution to $-N''(E)$. In the high-energy region ($30 \lesssim E \lesssim 80$ eV), $N'(E) = dN/dE$ was used to locate structure in $N(E)$. Reasons for this are given later in this paper.

Since much of the low-energy structure is associated with collective plasmon oscillations, one should note that for the free-electron gas, the plasma energy is given by[15]

$$\hbar\omega_p = \hbar\left(\frac{4\pi Ne^2}{m}\right)^{1/2}, \tag{3}$$

where N is the number of electrons per unit volume,

TABLE III. Molybdenum.

		A′	Energy loss (eV) A	B	C	D	E	E′	E″	F
Reflection ELS	This study		10.2 ±0.2		20.1 ±0.3	23.9 ±0.5	35.2 ±0.4	41.0 ±0.3	48.2 ±0.3	63.4 ±0.8
	Ref. 21		9.9		22.8				46.8	69.8
	Ref. 35		9.5		21.5					
	Ref. 34		10.1		22.4					
	Ref. 33[a]		10.3(GI)		20.2(GI)				43.8(GI)	61.0(GI)
			10.3(NI)		23.0(NI)				46.0(NI)	61.0(NI)
	Ref. 36	4.0	9.0		18	25.0				
uv optical	Ref. 11						32.4			
			9.5	10.4	19.8	24.4	34.6			
X-ray atomic energy levels	Ref. 25						34.8 ±0.4 $N_{\mathrm{II}},N_{\mathrm{III}}$			61.8 ±0.3 N_{I}
Calculated free electron $\hbar\omega_p$	Ref. 11					23.1				

[a]GI = Grazing incidence, NI = normal incidence.

TABLE IV. Tantalum.

		Energy loss (eV)										
		A′	A	B	C′	C	D	E	F′	F	G	H
	This study	4.1 ±0.4	8.2 ±0.3		12.5 ±0.3	18.0 ±0.2	20.5 ±0.3	26.7 ±0.4	32.7 ±0.4	37.4 ±0.4	46.5 ±0.5	
Reflection ELS	Ref. 21		9.4			19.6				38.7	48.8	72
	Ref. 33[a]		10.0(GI)			16.7(GI)				37.0(GI)	47.0(GI)	
			10.0(NI)			20.0(NI)				39.0(NI)	47.0(NI)	
	Ref. 34		10.4			20.4						
uv optical	Ref. 1							23.6				
			8.6	8.9		17.2	20.7	26.0				
X-ray atomic energy levels	Ref. 25							25.0 ±0.4 N_{II},N_{III}		36.4 ±0.4 O_{III}	44.9 ±0.4 O_{II}	71.1 ±0.5 O_{I}
Calculated free electron $\hbar\omega_p$	Ref. 11						19.7					

[a] GI = Grazing incidence, NI = normal incidence.

e is the electronic charge, and m is the electron mass. Assuming the s and d electrons are free, this equation results in plasmon energies around 20 eV (see Tables I–IV) for the transition metals considered here. The ideal-surface plasmon is predicted to occur at approximately $\hbar\omega_p/\sqrt{2}$.[16] It is also well known that an optical band may shift the free-electron plasma energy upwards or downwards depending upon the relative positions of the band and the plasma energy.[17] However, we shall see that these naive expectations cannot fully explain the rather complex collective behavior observed in the transition metals.

II. EXPERIMENTAL METHOD

The basic features of the experimental chamber have been previously described by Shen.[18] The present chamber differs in that non-normal incidence of the electron beam is used for the Auger-electron spectroscopy (AES) and ELS measurements. The energy analyzer used for both the AES and ELS is a double-pass cylindrical mirror analyzer (CMA) with retarding grids.[19]

High-purity transition-metal foils (0.002 to 0.005 in. thick) were electropolished and cleaned in methanol before being mounted in the experimental chamber. After reaching a base pressure of $P \leq 5\times10^{-10}$ Torr, the foils were outgassed at temperatures approaching their melting points by Joule heating. Pressures during final outgassing were $\lesssim 5\times10^{-9}$ Torr. With Mo, Nb, and Ta the above treatment created a clean-foil surface, as indicated by the Auger spectra. Vanadium, however, required additional sputter cleaning and annealing to about 800 °C to remove fractional surface coverages of phosphorus and sulfur. The vanadium Auger spectra then showed minimal carbon contamination ($\lesssim 5\%$).

The ELS spectra were taken with the CMA used in a preretarding mode to obtain sufficient energy resolution (±0.7 eV, limited by primary energy width). Each run consisted of three ELS traces $[N(E),\ N'(E)=dN/dE$, and $-N''(E)=-d^2N/dE^2]$, preceded and immediately followed by Auger analysis to monitor the surface cleanliness. In all of the results reported here, the Auger spectra showed $\lesssim 5\%$ contamination of the sample surface, with the major contaminants being carbon and oxygen. $N(E)$ was measured in a pulse counting mode, while the derivatives were taken by applying a small voltage modulation to the outer cylinder of the CMA and using lock-in techniques, in the usual manner of AES.[20] Several runs were made on each sample and the loss values reported are averages with standard deviations.

In addition, primary energies ranging from 250 to 1090 eV were used with essentially identical results in energy positions of observed structure. Also, it was noted that the spectra did not show a dependence on the angle of incidence (generally about 65° with respect to the foil normal), probably due to the polycrystalline nature of the sample area illuminated and the relatively wide angular acceptance of the CMA.

III. RESULTS

Sample spectra from the present work can be seen in Figs. 2–5. Energy-loss values (E) from this work are compared with those of previous investigators in Tables I–IV. Also included in these tables are x-ray atomic energy levels and calculated free-electron plasma energies. Features listed in columns A, B, C, and D of the tables are associated with plasmons following the optical results of Weaver *et al.*,[11,12] while columns labeled E, F, G, and H correspond to core-excitation energies. Generally good agreement with previous investigations is shown for each metal.

As mentioned previously, structure positions in the low-energy region were determined from $-N''(E)$. Assuming that losses in this region arise from collective excitations or interband transitions, both of which cause peaks in the loss function [and thus $N(E)$][9,11,12] this procedure seems valid. In the high-energy region, the first derivative $N'(E)$ was used to locate structure. At the threshold for excitation of a core electron, one expects to see a possibly broadened step increase in $N(E)$.[21] The point of inflection of this increase can be located by the corresponding peak in $N'(E)$.

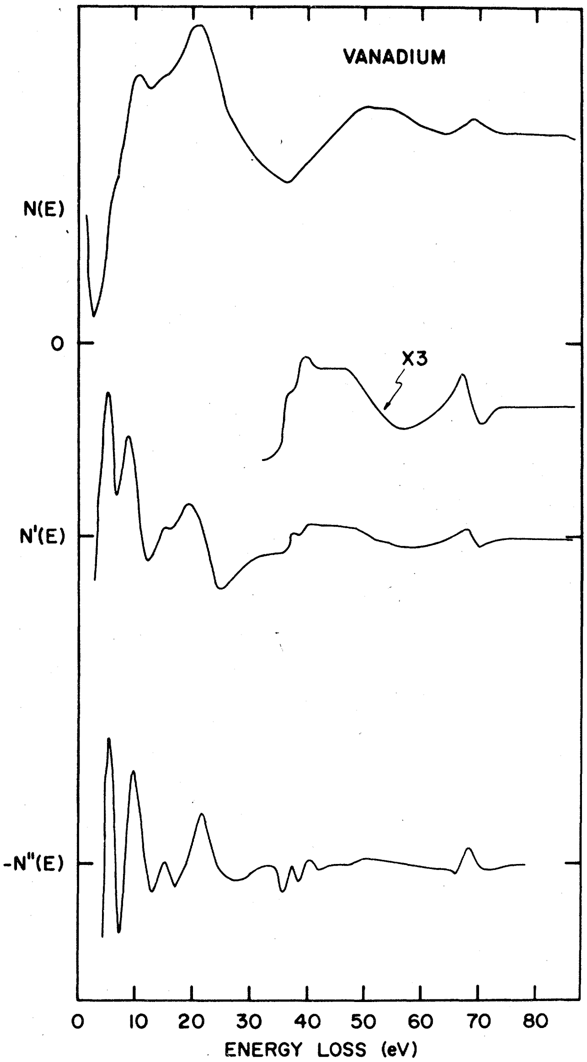

FIG. 2. Sample electron-energy-loss spectra for vanadium measured with an incident electron energy of 690 eV.

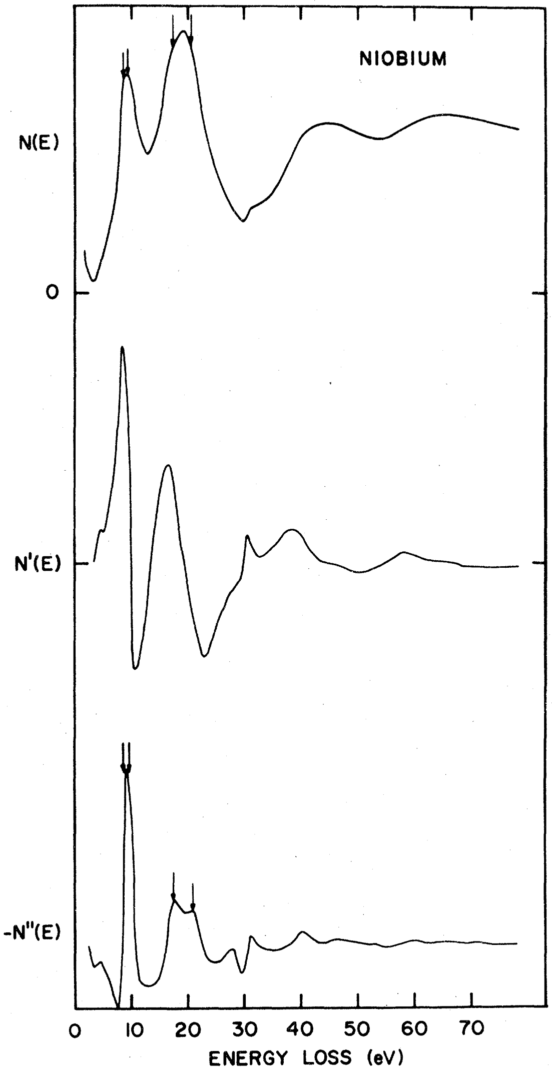

FIG. 3. Sample electron-energy-loss spectra for niobium measured with an incident electron energy of 690 eV. Arrows indicate plasmon energies determined from uv optical work by Weaver *et al.* (Ref. 12).

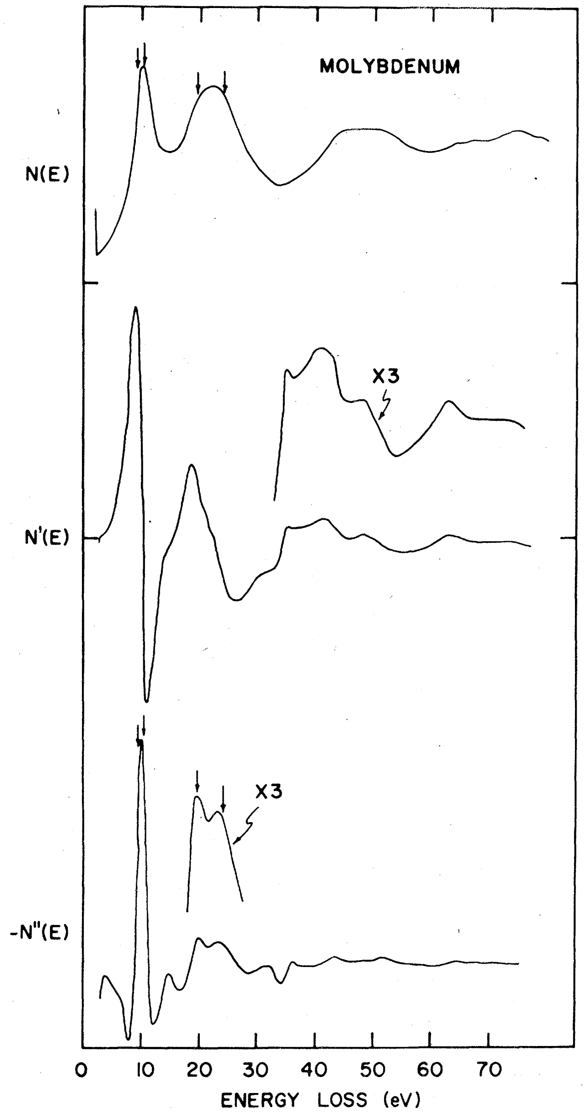

FIG. 4. Sample electron-energy-loss spectra for molybdenum measured with an incident electron energy of 690 eV. Arrows indicate plasmon energies determined from uv optical work by Weaver *et al.* (Ref. 11).

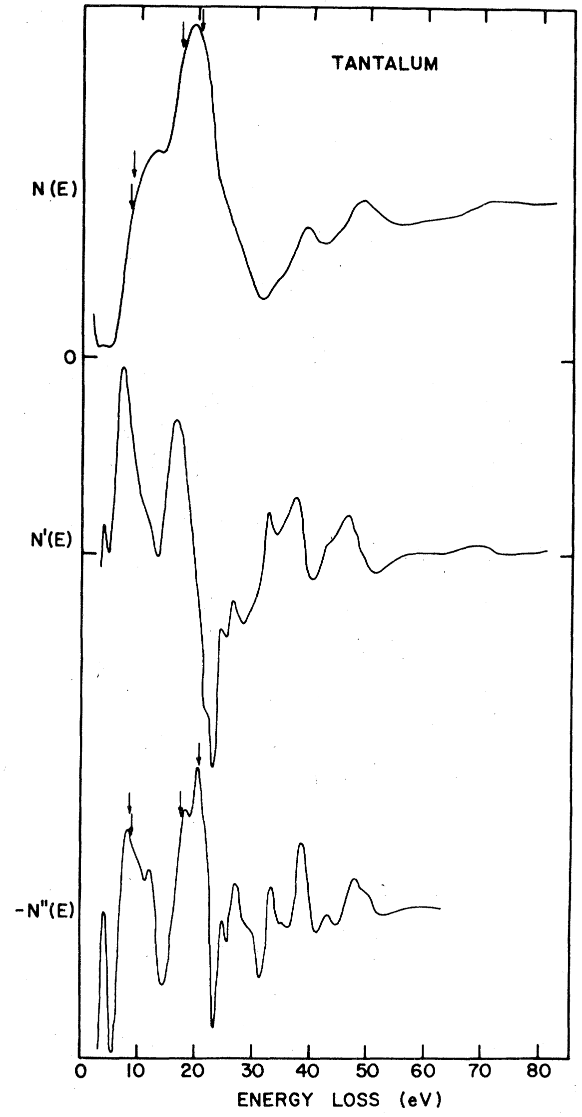

FIG. 5. Sample electron-energy-loss spectra for tantalum measured with an incident electron energy of 690 eV. Arrows indicate plasmon energies determined from uv optical work by Weaver *et al.* (Ref. 11).

IV. DISCUSSION

A. Low-energy region ($E \lesssim 30$ eV)

It appears that most of the low-energy structure in the present study (and previous work by other investigators) can be identified with the plasmons (volume and surface) and lowered plasmons (volume and surface) reported by Weaver, Lynch, and Olson[11,12] in uv optical studies on these same materials. The volume and surface loss functions of niobium from Ref. 12 are shown in Fig. 1. In this figure the solid line represents the volume loss function, the dotted, the surface loss function. Note that the high-energy peak in the surface loss function by no means occurs at $\hbar\omega_p/\sqrt{2}$, if $\hbar\omega_p$ is identified with the upper peak in the volume function. Further, *each* curve has a lower energy peak, referred to by Weaver *et al.*[11,12] as the "lowered plasmon". Criteria for the identification of these lowered structures as plasmon-loss peaks are given by Weaver *et al.*[11,12] Note the similarity of the loss functions (Fig. 1) with $N(E)$ for niobium given in Fig. 3. In Figs. 3–5, the locations of the four plasmons determined by Weaver *et al.*[11,12] are indicated by small arrows. The agreement is obvious. The upper volume and surface plasmons are resolved in $-N''(E)$ in each of the four metals. The lowered volume and surface plasmons are resolved only in vanadium. This is believed due to the close proximity in energy of the volume and surface plasmons of the lowered branch in niobium, molybdenum, and tantalum. In vanadium, other investigators have proposed such mechanisms as multiple and combination plasmon losses[14] for the losses listed in columns C and D. Also, several investigators[10,18,22–24] have attributed losses in columns A and B to various interband mechanisms. We feel that these explanations are less likely in view of the optical results which give definite criteria[11,12] for plasmon identification.

The two sets of plasmons adequately explain the low-energy regions of vanadium, niobium, and molybdenum. In tantalum, however, extra structure in $-N''(E)$ is apparent at 4.1 and 12.5 eV. These peaks are not reported by previous investigators, although an unidentified structure appears at about 13 eV in the loss functions of tantalum given by Weaver *et al.*[11] We can propose no definite mechanisms for these structures. The 4.1 eV peak may be associated with the $O_{\mathrm{IV,V}}$ level (given as 5.7 eV by Bearden and Burr,[25] whose notation is followed here and in Tables I–IV) but the energy agreement is not good. Also, similar low-lying levels are not observed in any of the other three materials. The 12.5 eV loss is perhaps a combination of the 4.1 and 8.2 eV losses, but this cannot be substantiated from the present results except for the obvious energy agreement. Neither the 4.1 or the 12.5 eV loss seems to be surface related, in that tantalum samples showing considerable oxygen contamination display structure at the same energies. Interband transitions also remain a possibility.

B. High-energy region ($30 \leq E \leq 80$ eV)

Most of the structure observed in the high-energy region is believed to arise from core-level excitations, and therefore x-ray atomic energy levels[25] are helpful in identification. Our core excitation identifications can be seen in Tables I–IV in columns labelled E, F, G, and H. The identifications are basically in agreement with the investigators quoted in the tables. In certain instances (the 41.9 eV loss of Ref. 23 in vanadium and the 46.8 eV loss of Ref. 21 in molybdenum), we have shifted losses reported previously as core levels to unidentified primed columns in the tables because of their energy values are actually quite far from reported x-ray levels.[25] These particular losses were observed in the present study in *addition* to losses lying nearer the core-level energies. Double scattering losses have been proposed in some cases (the 67.4 eV peak of vanadium[10]) as mechanisms for structure in the high-energy region, in spite of the fact that the loss occurs very near a core-level energy. However, because we observe structure near all of the accessible core levels in each of the four materials, we feel confident in identifying peaks with core levels when energy agreement is adequate.

Further interpretation of the high-energy region features is complicated somewhat by the extra structure which cannot be directly related to core-level excitations. Such additional structure is not unexpected, since it has been observed in previous ELS work (see Tables I–IV) and in the x-ray work of Sonntag *et al.*[26] and Haensel *et al.*[27] on these same materials. Many interpretations have been assigned to this additional structure. Shen[18] attributed additional structure above the $M_{\mathrm{II,III}}$ level in vanadium to peaks in the density of empty states above the Fermi level, in moderately good agreement with the band calculations of Papaconstantopoulos *et al.*[28] However, one might question why such structure is not also seen above the M_{I} core level. Indeed, agreement with band-structure calculations[29] is not obvious for the additional structure in niobium, molybdenum, and tantalum. Misell and Atkins[22] suggest that extra vanadium structure may be due to splitting of the excited state through an exchange interaction between the unfilled d shell and the 3-p hole. Similar structure in the absorption spectra of rare-earth metals has been explained in this manner.[30] Zashkvara *et al.*[31] proposed yet another mechanism for similar structure in the second and third transition-metal series which does not agree well with core-level energies. This explanation invokes "ionization-plasma" processes which involve the ionization of the $4p$ level with a transition to the $4d$ state accompanied by the excitation of a lowered plasmon (of the type discussed earlier). Energy agreement is not particularly impressive, however, and not all of the extra structure can be accounted for in this manner. Finally, Szalkowaki *et al.*[24] proposed momentum-conserving interband transitions of the type described by Viatskin[32] to explain the additional structure above the $M_{\mathrm{II,III}}$ level in vanadium.

The particularly rich structure of tantalum is worthy of closer examination. Here, separation of the collective oscillations and the core-level excitations is much smaller than in the other three materials. In fact, the $N_{\mathrm{VI,VII}}$ core levels at 26.7 eV lie on the high-energy shoulder of the upper volume plasmon peak. In spite of the rapidly changing background due to the plasmon, these low-lying core levels are quite apparent in $N'(E)$ (see Fig. 5). In addition, one observes the O_{III} (37.4 eV) and O_{II} (46.5 eV) levels in $N'(E)$. The extra structure in tantalum, that is, the E' peak at 32.7 eV and the shoulder at about 42 eV (not included in Table IV) is unusual in that it seems to lie *below* the core level with which it is associated. In addition, it was observed that these unidentified extra structures seemed to be surface specific, in that oxidized tantalum surfaces did not exhibit either loss peak (while all other high-energy peaks remained unchanged).

V. CONCLUSIONS

The above results show that reflection ELS measured in the manner of this experiment is an extremely valuable tool for studying the electronic properties of the transition metals. Energy-loss values so determined are in good agreement with previous investigations, including ultraviolet, x-ray, and other ELS studies. The advantage of using derivative techniques in this energy range ($0 \lesssim E \lesssim 80$ eV) is apparent in the greater number of loss structures revealed. In every case, the amount of structure shown by the present study is at least as much as that shown in any previous work. Note that in the well-studied case of vanadium, while more structure is seen than in any previous *single* study, no previously unobserved structure appears.

Finally one should note that the plasmon energies reported here (and by the other investigators quoted in Tables I–IV) are *not* in agreement with very low plasmon energies (6 eV in niobium) recently obtained by parameterization of infrared optical-absorption measurements.[7,8] It appears that although the transition metals, and their related A-15 compounds, display Drude behavior in the very low-energy region ($0.16 \leq \hbar\omega \leq 0.62$ eV), it is difficult to use this data to accurately predict plasmon energies which lie far above the experimental energy range.

ACKNOWLEDGMENTS

This work was supported by the U.S. Department of Energy, Office of Basic Energy Sciences, Materials Sciences Division. We thank Professor D. W. Lynch for permission to reproduce Fig. 4 from Ref. 12. The donation of the experimental chamber by Bell Laboratories and the receipt of a Cottrell Grant from Research Corporation are gratefully acknowledged.

---

[1] D. Dew-Hughes, Cryogenics 15, 435 (1975).
[2] W. L. McMillan, Phys. Rev. 167, 331 (1968).
[3] S. K. Sinha and B. N. Harmon, in *Superconductivity in d- and f- Band Metals*, edited by D. H. Douglass (Plenum, New York, 1976), p. 269.
[4] J. Ruvalds and L. M. Kahn, Phys. Lett. (to be published).
[5] H. Fröhlich, J. Phys. C 1, 544 (1968).
[6] W. E. Pickett and P. B. Allen, Phys. Rev. Lett. A 48, 91 (1974); Phys. Rev. B 13, 1473 (1976).
[7] L. F. Mattheiss, L. R. Testardi, and W. W. Yao, Phys. Rev. B 17, 4640 (1978).
[8] I. Tüttö, L. M. Kahn, and J. Ruvalds (unpublished).
[9] H. Froitzheim, in *Electronic Spectroscopy for Surface Analysis*, edited by H. Ibach (Springer-Verlag, Berlin, 1977), p. 205.
[10] C. Wehenkel and B. Gauthé, Phys. Status Solidi B 64, 515 (1974).
[11] J. H. Weaver, D. W. Lynch, and C. G. Olson, Phys. Rev. B 10, 501 (1974).
[12] J. H. Weaver, D. W. Lynch, and C. G. Olson, Phys. Rev. B 7, 4311 (1973).
[13] P. E. Best, Proc. Phys. Soc. London 80, 1308 (1962).
[14] G. W. Simmons and A. J. Scheibner, J. Appl. Phys. 42, 693 (1972).
[15] C. Kittel, *Introduction to Solid State Physics*, 4th ed. (Wiley, New York, 1971), p. 270.
[16] R. H. Ritchie, Phys. Rev. 106, 874 (1957).
[17] C.B. Wilson, Proc. Phys. Soc. London 76, 481 (1960).
[18] L. Y. L. Shen, Surf. Sci. 66, 239 (1976).
[19] P. W. Palmberg, J. Electron Spec. Related Phenom. 5, 691 (1974).
[20] C. C. Chang, in *Characterization of Solid Surfaces*, edited by P. F. Kane and C. B. Larrabee (Plenum, New York, 1974), p. 509.
[21] M. J. Lynch and J. B. Swan, Aust. J. Phys. 21, 811 (1968).
[22] D. L. Misell and A. J. Atkins, Philos. Mag. 27, 95 (1973).
[23] J. L. Robins and J. B. Swan, Proc. Phys. Soc. London 76, 857 (1960).
[24] F. J. Szalkowski, P. A. Bertrand, and G. A. Somorjai, Phys. Rev. B 9, 3369 (1974).
[25] J. A. Bearden and A. F. Burr, Rev. Mod. Phys. 39, 125 (1967).
[26] B. Sonntag, R. Haensel, and C. Kunz, Solid State Commun. 7, 597 (1969).
[27] R. Haensel, K. Radler, B. Sonntag, and C. Kunz, Solid State Commun. 7, 1495 (1969).
[28] D. A. Papaconstantopoulos, J. R. Anderson, and J. W. McCaffrey, Phys. Rev. B 5, 1214 (1972).
[29] L. L. Boyer, D. A. Papaconstantopoulos, and B. M. Klein, Phys. Rev. B 15, 3685 (1977).
[30] J. L. Dehmer, A. F. Starace, U. Fano, J. Sugar, and J. W. Cooper, Phys. Rev. Lett. 26, 1521 (1971).
[31] V. V. Zashkvara, M. I. Korsunskii, V. S. Red'kin, and K. Sh. Chokin, Sov. Phys. Solid State 14, 1891 (1973).
[32] A. Ia. Viatskin, Sov. Phys. Tech. Phys. 3, 2038 (1958); Sov. Phys. Tech. Phys. 3, 2252 (1958).
[33] V. V. Zashkvara, M. I. Korsunskii, U. S. Red'kin, and V. E. Masyagin, Sov. Phys. Solid State 11, 3083 (1970).
[34] H. R. Apholte and K. Ulmer, Phys. Lett. 22, 552 (1966).
[35] Y. Ballu, J. Lecante, and H. Rousseau, Phys. Rev. B 14, 3201 (1976).
[36] M. I. Korsunskii, Ya. E. Genkin, S. M. Chanyshev, and E. V. Tsveiman, Sov. Phys. Solid State 16, 557 (1974).